

**2019 NDIA GROUND VEHICLE SYSTEMS ENGINEERING AND TECHNOLOGY  
SYMPOSIUM  
< MATERIALS & ADVANCED MANUFACTURING (M&AM) > TECHNICAL SESSION  
AUGUST 13-15, 2019 - NOVI, MICHIGAN**

**Test the Corrosion Effect on High Hard Steel Armor MIL-DTL-46100  
Coated with Stellite 6 Applied by Direct Energy Deposition Method**

**Ian J Toppler<sup>1</sup>, Daniel C Schleh<sup>2</sup>, Lieutenant Colonel  
Claudio Gutierrez Romero<sup>3</sup>**

<sup>1,2</sup> Army Futures Command – Materials Division, Warren, MI

<sup>3</sup>Chilean Army, Santiago, Chile

**ABSTRACT**

*The U.S. Army - GVSC Materials Characterization and Failure Analysis team conducted a preliminary study in FY18 to address the issue of galvanic and pitting corrosion of U.S. Army ground vehicle system (GVS) structural surfaces. The objective of this study was to develop a permanent coating solution to supplement the existing corrosion protective coating of zinc rich primer and CARC paint, and extend the lifecycle of the armor. Twenty-five permanent, 0.1 inch layer, additively manufactured (AM) coated coupons of deposited Stellite 6 cobalt alloy on MIL-STD-46100 High Hard (HH) armor steel blocks were produced for cyclic testing using an un-optimized set of parameters. These coupons were subjected to a twenty-four week study in accelerated corrosive conditions of a fog spray chamber alongside primer-CARC coated and uncoated coupons. The resulting study showed no signs of pitting corrosion in the surface of the AM coated coupons, and minimal galvanic corrosion.*

**Citation:** I. Toppler, D. Schleh, C. G. Romero, “Test the Corrosion Effect on High Hard Steel Armor MIL-DTL-46100 Coated with Stellite 6 Applied by Direct Energy Deposition Method”, In *Proceedings of the Ground Vehicle Systems Engineering and Technology Symposium (GVSETS)*, NDIA, Novi, MI, Aug. 13-15, 2019.

## **1. INTRODUCTION**

The use of Direct Energy Deposition (DED) technologies to modify existing surfaces of metallic structures to resist the effects of corrosion is one of the Army’s primary areas of research in metal additive manufacturing. A corrosion study assessing the behavior of MIL-DTL-46100 high

hard armor steel coated with a powder metal alloy, using the DED technology, is of particular interest to the Department of Defense (DoD). The Characterization and Failure Analysis team of the GVSC-Materials Division has conducted prospective research directed towards practical applications of the DED technology related to the field of preventing and repairing pitting corrosion. Pitting repaired through traditional procedures are conducted by removing the corrosion and refilling the hole with a weldment. This is a temporary fix, which commonly results in heat affected zones

(HAZ) that reduce armor quality beneath and around the repair. Such repairs can become very risky and expensive in critical areas, such as near the turret ring of vehicles like the LAV 25. Such repairs can result in warpage of the structure if the heat input is too great, and cost a considerable amount to ensure ring tolerances again meet specifications.

Through the implementation of DED technology, the capability to conduct repairs and prevent corrosion development may result in a significantly reduced cost and risk. A benefit of the DED repair process over weldment repair is a significantly smaller amounts of heat can be imparted with the DED across the localized area, which reduce effects on the surrounding microstructure. A study with the cobalt based alloys Stellite 6 was selected for this investigation due to its wear and corrosion resistance [1]. The Stellite materials commonly have an similar hardness to the armor MIL-DTL-46100 substrate. Evaluation of corrosion resistance through an accelerated aging processes, such as a salt fog spray chamber is a common analysis method, which was employed in this study to compare the corrosion resistance of the DED coating verse currently used protective coatings.

## 2. PRELIMINARY STUDY DETAILS

The base coupons were made out of a half inch thick high hard steel armor (MIL-DTL-46100) plate. Surface hardness of this material is between 49-54 HRC (477 and 534 BHN). This study consisted of a total of 75 test coupons. Each coupon was rectangle shaped, sized 25.4 mm by 50.8 mm by 13mm of which: 25 pieces remained bare uncoated metal, 25 pieces covered with a MIL-DTL-64159-Type 2 CARC paint and zinc rich primer coating, and 25 pieces covered with a two layer coating of Stellite 6 powder. The coupons were placed in the GVSC Fuels & Lubricants Laboratory salt fog spray chamber for 24 weeks. The percent salinity was maintained within the range of 4.5 to 5.4, and pH of the chamber ranged from 6.7 to 7.1. A single coupon of each type was

removed and measured for mass loss and development of corrosion product each week.



Figure 1. Image of the uncoated, primer-CARC, and DED coated test coupons.

### 2.1. Material Specifications

Stellite alloys are resistant to wear, galling, corrosion, and retain these properties at high temperatures [2]. Their natural wear resistance is primarily the result of the hard chrome rich carbide phase dispersed in a CoCr alloy matrix. See Figure 2 [3]. Stellite 6 is known by the Army for its general- purpose wear resistance applications. Stellite 6 used in this study was manufactured by Kennametal. Stellite 6 has excellent resistance to many forms of mechanical and chemical degradation over a wide temperature range, and is stated by the manufacturer to retain a reasonable level of hardness up to 500C (930F). It is also stated to have good resistance to impact and cavitation erosion.

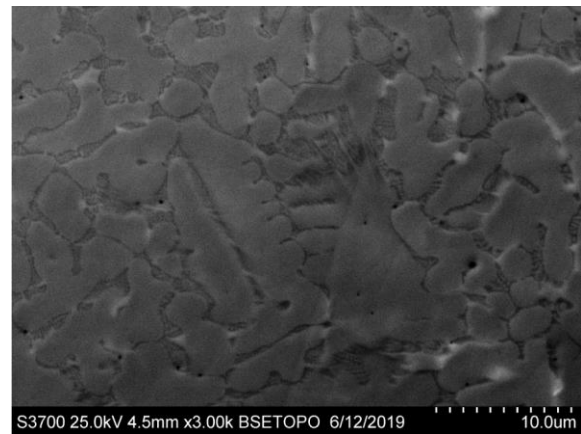


Figure 2. Scanning electron microscope BSE image of deposited Stellite 6, at 3000x magnification. Carbide structure can be seen within CoCr alloy matrix.

In regards to corrosion, the typical electrode potential in sea water at room temperature is -0.25 V (SCE). Like stainless steels, Stellite 6 corrodes primarily by a pitting mechanism and not by general mass loss in seawater and chloride solutions. Its mass loss in sea water is below 0.05mm per year at 22C. [4] The chemical composition, hardness, density, and melting range can be seen in Table 1, as stated by the manufacturer.

Table I: Chemical Composition of Stellite 6.

Composition				
Co	Cr	W	C	Other
Base Material	27 - 32	4 - 6	0.9 - 1.4	Ni, Fe, Si, Mn, Mo

Table II: Mechanical properties of Stellite 6.

Hardness	Density	Melting Range
36-45 HRC	8.44 g/cm <sup>3</sup>	2340-2570 °F
380-490 HV	0.305 lb/in <sup>3</sup>	1285-1410 °C

**2.2. Coupon Preparation**

The coupon preparation process for both the preliminary study and optimization process are the same. The substrate test plate, prior to sectioning coupons, shall be in the as-heat treated condition, with the surface not pickled. The surface hardness of the test plate was verified to be within the specified hardness range of MIL-DTL-46100. The top and bottom surfaces were checked to ensure they were free of surface defects. Base coupons are sized to 25.4 mm by 50.8 mm by 13 mm, through the use of a water jet cutting method. Before deposition, the coupons were suitably cleaned and sand blasted. Each coupon was massed before and after the Stellite coating process, to determine the

amount of mass added from the deposition. The Stellite 6 coupons are coated with a double layer on the top surface and all 4 sides, leaving bottom uncoated to measure galvanic interactions. The coupons coated with primer-CARC paint were also only coated on the top and sides for comparability. After the deposition process was complete, the coupons were polished to an 80 grit finish to make the identification of pitting clear during the salt spray analysis. The uncoated specimens had an initial average mass of 130.404 g, and with a standard deviation of 0.441 between the coupons. The coating of Stellite 6 added an additional average of 75.229 g to the uncoated specimens, using the non-optimized deposition parameters.

**2.3. Coating Method**

The DED coating for the HH coupons were produced with the DM3D 405D deposition system. The Stellite 6 was applied in a powder form, with a particle size range of 30 to 150 microns. The powder was preheated with an open atmosphere oven at 400 degrees Fahrenheit, for 10 minutes, before being loaded into the DM3D powder hopper. The powder was delivered to the substrate during the DED process through the use of a grade 5 argon gas flow system. The first layer used a powder flow rate of 28.4 g/min and a laser power input of 2 kW. The second layer used a flow rate of 17.7 g/min and an input of 1 kW. The head movement speed for was 880 mm/min for the first layer and 340 mm/min for the second layer. The two layers were completed in an alternating transverse-longitudinal pattern with a 2 mm laser spot size, and a 1.25 mm offset from the center of the beam for each overlapping pass, in each layer. The DED process was conducted in an open air environment, with a shield gas provided in addition to the powder carrier gas to protect the melt pool during deposition. A cross section of the unfinished deposition can be seen in Figure 3 below. Each side of the coupons were designated, as seen in the right side of Table III.



Figure 3. The before and after image of an uncoated and coated coupon can be seen in this image.

Table III. The identification of the sides and their geometries can be seen in the corresponding chart to the right.

Surface	Length	Height	Identification
Side 1	2 inches	1 inch	Back Side (uncoated all)
Side 2	2 inches	½ inch	Upper side (Coated/painted)
Side 3	1 inches	½ inch	Right Side (Coated/painted)
Side 4	2 inches	½ inch	Bottom Side (Coated/painted)
Side 5	1 inches	½ inch	Left Side (Coated/painted)
Side 6	2 inches	1 inch	Front side (Coated/painted)

### 2.4. Corrosion Chamber - Data Collection

Three sets of corrosion coupons were placed into the corrosion chamber for the 4032 hours run. The operating temperature was held at 35°C with a salt spray composition target of 5% NaCl. The functional test time between coupon evaluations was 167 hours, 45 minutes, per week. This allowed for a weekly 15 minute coupon removal period and maintenance cycle. Each coupon was placed in the chamber with Side 6 at a 75 degree incline, from horizontal. Side 6 was the target to analyze the development of pitting corrosion, while the interface between the side 1 and sides 2 through 5 were evaluated for galvanic corrosion.

The samples were tested in accordance with (IAW) ASTM B117-16 Standard Practice for Operating Salt Spray (Fog) Apparatus using a Q-Fog CCT600 salt fog apparatus. After each weekly extraction, each coupon was lightly washed with water and placed in a desiccator to await further analysis.

### 3. RESULTS

As can be seen from Figures 4, 5, and 6, the development of corrosion on the coupon surfaces can be seen in weekly order of 1, 12, and 24, from top to bottom. The unprotected surfaces (side 1) of each specimen type demonstrated consistent progression of corrosion build up in equal measure. The corrosion resistance of the painted coupon were comparatively superior to the uncoated coupons. However, indications of pitting under the front painted surfaces of side 6 were noted in the week 8. The front surface (side 6) of the painted coupons began demonstrated considerable pitting around week 9. Also during week 9, the interfacing edges of the primer-CARC and substrate on side 1 began demonstrating a progressive increase in corrosion incursion.



Figure 4. Uncoated substrate specimens.

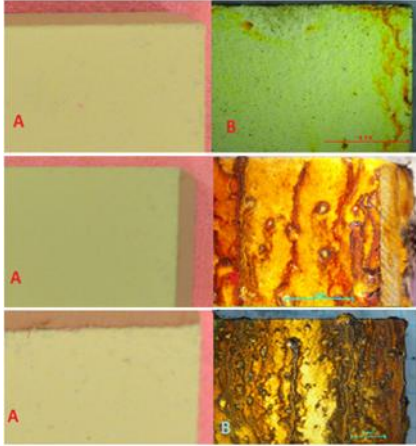


Figure 5. CARC paint and primer specimens.

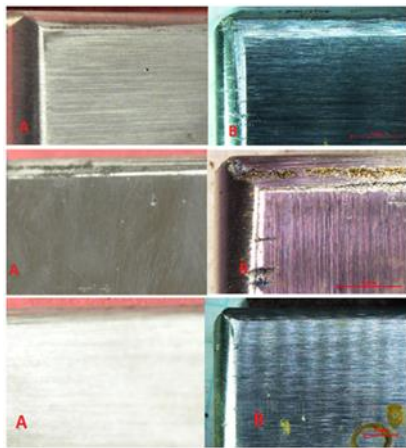


Figure 6. Stellite 6 specimens

In relation to the painted coupons, the back side (side 1) of the coated coupons demonstrated a similar pattern of corrosion build up. Upon the coated surfaces, a marginal amount of corrosion progression nucleated from the manufacturer defects, but appeared to have no ingress into the surface. The polished surface of the coated specimens were effectively unblemished with the exception of some dried water droplets. There were no signs of surface cracks upon inspection or penetrating defect that could suggest a failure of the coating to prevent ingress of the corrosive environment to the substrate surface during the testing.

### 3.1. Mass Loss

Once the coupons were extracted, the corrosion product was removed through the ASTM B117 procedure, using a solution consisting of 1000 mL of hydrochloric acid, 1000 mL of reagent grade water, and 10 g of hexamethylene tetramine. Once rinsed from that solution, the coupons were massed, reimaged, and sectioned to assess the depth of the pitting and galvanic corrosion in their respective surfaces. A table denoting the trending mass lost, in grams, can be seen in Figure 7.

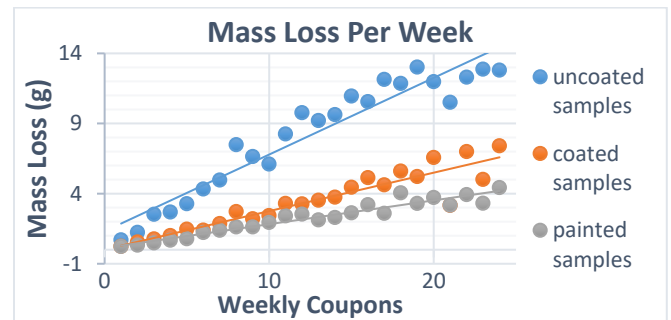


Figure 7. Chart of mass loss by week for each specimen type.

The coated specimens were cross sectioned from week 1, 6, 12, 18, and 24, and visually inspected to evaluate the locations of the mass loss, as seen in Figure 9. As seen in image A of Figure 9, there was some overlap of the Stellite 6 deposition along the back side of the coupon, which varied slightly depending on the coupon orientation during the deposition process. Mass loss was noted across the surface of the back side and interface of the Stellite 6 and MIL-DTL 46100 substrate. However, considerably more mass loss was noted at the interface when compared to the painted coupons.

The week 1 and 6 coupons appeared to experience uniform mass loss across the surface and at the interface. However, the loss of material became apparent in the specimen at week 12, where mass loss was more pronounced along one of the interfaces. It can also be seen that this loss of mass at the interface was not uniform about the entire coupon. The cross sections of Week 18 and 24

demonstrated loss across the entire back surface, and Week 24 showed a considerable amount of loss in one location of the interface where Image E of Figure 9 was taken.

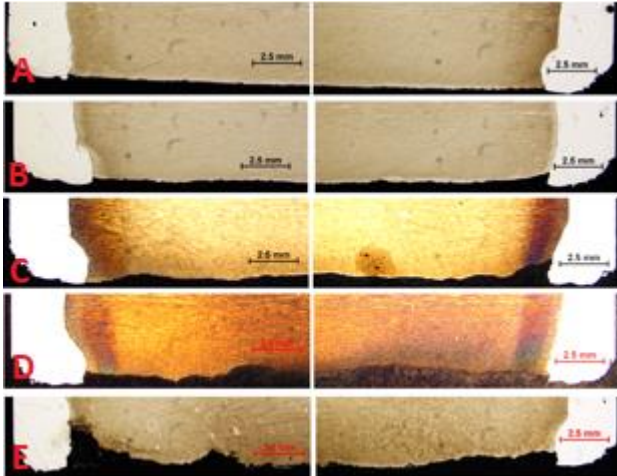


Figure 9. The cross sectional stereographs demonstrating the amount of mass loss from the Stellite 6 coated coupons of Week 1 (A), Week 6 (B), Week 12 (C), Week 18 (D), and Week 24 (E).

### 3.2. Galvanic Corrosion in the Coated Specimens in Salt Water

It was observed that the coated coupons produced a greater mass loss than that of the painted coupons throughout the study, and it was assessed that there was a consistent amount of material loss occurring each week in the proximity of the substrate/Stellite 6 coating interface, verse the rest of the side 1 surfaces.

This pattern of material loss persisted through each weeks' specimen and was noted on every interfacing edge. The repetition of the characteristic led to a presumption that this length of area was consistent with a heat affected zone from the DED process, which was further confirmed by the hardness measurements, and not primarily attributable galvanic corrosion. The length of this affected area averaged  $\approx 0.12$  inches ( $\approx 3$  mm) and extended up to 0.2 inches (5 mm) across the back surface of side 1 from the coating in some specimens. This distinctive area, as seen marked by

a red line in Figure 10, demonstrates the depth of the HAZ in relation to this region of material loss.

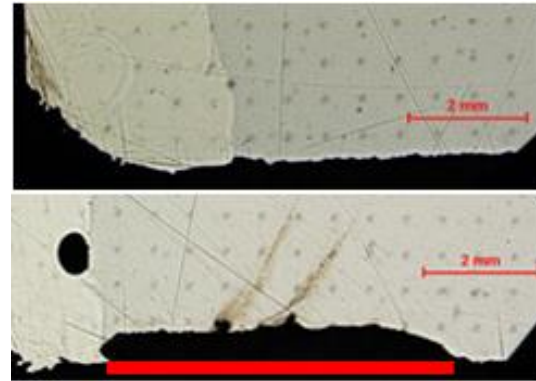


Figure 10. Cross sections from sample of Stellite 6 coating from week 1 (left) and week 20 (right).

Each of the specimens were inspected for the existence of galvanic corrosion on the exposed back side of the specimens (Side 1). Depending on the manufacturer, the electrical potential for this steel substrate ranges from -0.50 to -0.42 V [5]. The electrical potential for Stellite 6, according to the manufacturer, is -0.25 V [4]. This provides a difference in electric potential activity between 0.25 V and 0.17 V.

### 3.3. Hardness Mapping

Vickers hardness mapping was conducted in accordance with (IAW) ASTM E 92. Six specimens were produced and mapped for comparison. The first specimen was a cross section of an uncoated and unaltered base metal coupon. The other specimens consisted of a cross section from the following coated test coupons; Week 1, 6, 12, 18, and 24.

Hardness measurements were conducted to evaluate the deposition and its heat effects on the armor substrate. The mapping of the uncoated substrate can be seen in Figure 11. The uncoated substrate showed a relatively uniform hardness mapping, within the MIL-DTL-46100 specified 49-54 HRC (498 to 577 HV), with an average of 52 HRC (542 HV).

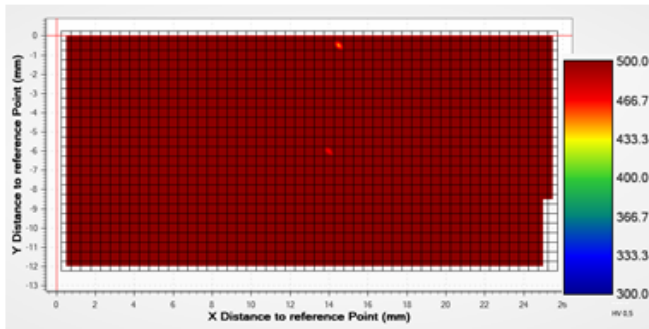


Figure 11. Vickers hardness map of the cross sectioned MIL-DTL-46100 substrate coupon. Areas in red represent hardness values greater than 498 HV ( $\approx$ 49 HRC).

The coated specimens demonstrate a consistent hardness mapping, as seen in Figure 12. There were two primary effects noted on the substrate from the coating process. The first resulted in a softened microstructure which penetrating from the coating interface to a depth of 0.12 inches ( $\approx$ 3 mm) in the sides and roughly 0.08 inches (2 mm) in the front surface of side 6. This area had an average hardness of 33 HRC (322 HV). The microstructure of this area of reduced hardness was observed to have a larger grain size than that of the core substrate which retained much of its hardness. The core, however, was observed to have dropped in hardness, to an average 38 HRC (371 HV). Which is 11 HRC below the minimum MIL-DTL-46100 specification.

Deposited Stellite 6 coating hardness ranged 50 to 53 HRC (510 to 555 HV), with a 52 HRC (538 HV) average. Exceeding the stated values by the manufacturer. The areas where there is only white space in Figure 12 represent the locations of porosity or cracks at or near the indent location, and no valid measurement could be recorded.

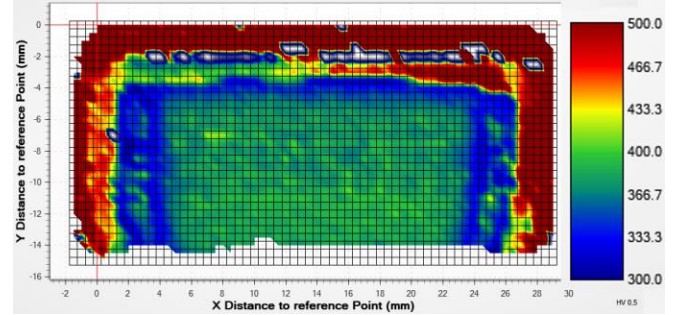


Figure 12. Vickers hardness map of week 6 Stellite 6 cross section. Areas in red represent hardness values greater than 498 HV ( $\approx$ 49 HRC). The areas in blue represent hardness values between 300 HV to 350 HV. The areas in green/yellow represent the transition between 351 HV and 497 HV.

### 3.4. Microstructural Effects

Similar to welding procedures, The DED process resulted in a change to the microstructure beneath the substrate surface. Commonly known as a heat affected zone (HAZ). The average depth of the HAZ was measured across the length of the front layer cross section (side 6), which can be seen in Figures 13 and 14. The depth was found to range between 0.07 inches and 0.09 inches in depth. With an average of 0.08 inches.

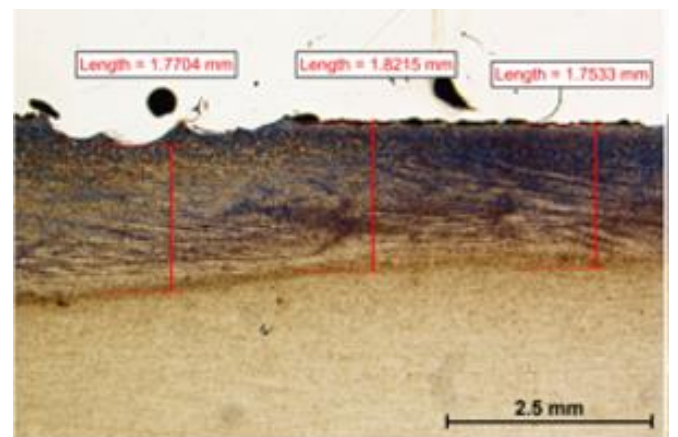


Figure 13. Micrograph of cross sectioned Week 6 coated coupon, where HAZ were measured.

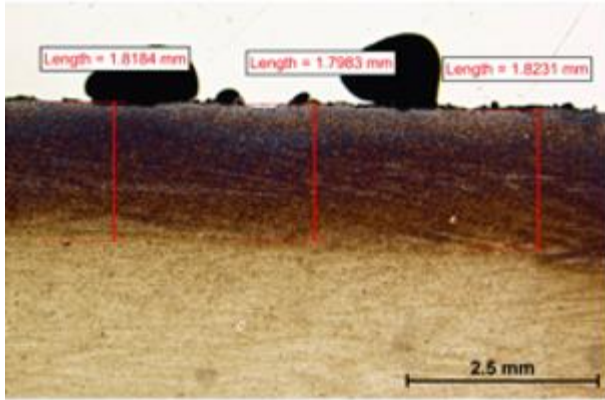


Figure 14. Micrograph of cross sectioned Week 6 coated coupon, where HAZ were measured.

The left and right surfaces (sides 2 and 4) averaged a maximum HAZ depth  $\approx 0.12$  inches ( $\approx 3$  mm) and extended up to 0.2 inches (5 mm) in some sections. Sides 3 and 5 were not measured as a part of this study, and will be taken into considered in the optimization process going forward.

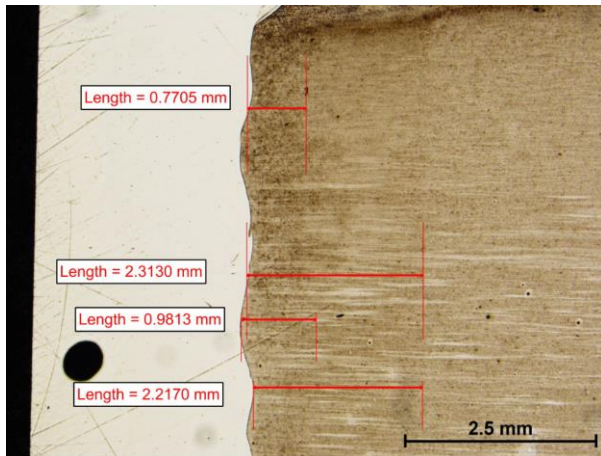


Figure 15. Micrograph of side 2 cross sectioned Week 6 coated coupon, where HAZ were measured.

#### 4. Process Optimization

There are a large number of factors ranging in importance and relevance to creating the resulting features and properties in any deposition. The primary factors that control heat input, as-well-as the creation of defects, in the deposition and

substrate are; laser intensity, beam spot size distribution, traversing speed of the beam across the deposition site, the amount of beam overlap between the passes, time between reheats, and the rate of powder being deposited.

As a result of this study, the optimization process requires a focus on three primary improvements.

1. Reduction of the heat effects across the entirety of the substrate core
2. Reduction of the depth of the HAZ
3. Removal of defects in the deposition layer

Each of these improvements may be achievable while still maintaining the corrosion and wear protection, through the manipulation of the parameters listed above. Since the wear of the armor surface is not as much of a concern as corrosion, a reduction in the deposition thickness may relieve each of these issues. A reduction in the amount of powder deposited will reduce the amount of required heat input per pass. This will also allow for a reduction in the traversing speed of the beam across the deposition site, which has been shown in prior experimentation conducted at GVSC to reduce the size and amount of porosity. The target layer thickness going forward would be to reduce the current layer thickness of the deposition from 0.1 inches (2.54 mm) to 0.05 inches (1.27mm) or less.

Variance in the deposition quality when comparing the front surface and the side surfaces was noted during this study, and demonstrates that the geometry of the surface to be deposited on plays a role in the deposition quality and effects. Which is to be expected and accounted for during the optimization process.

The reduction of powder, heat input, and traversing speed of the beam are expected to reduce the turbulence of the applied deposition process. This is expected to reduce the porosity that was observed within this study and improve or resolve the lack of fusion to the substrate surface.



## 5. CONCLUSION

The objective of this study was to determine the extent to which the DED coating could resist a corrosive environment and incursion of pitting through the surface to protect the steel substrate. The specified pass/fail criteria for the coating was determined by if the coating performed better or equivalent to the currently used CARC coating in protecting against pitting. The Stellite 6 coatings demonstrated a significantly improved protection to the steel substrate against the environmental conditions over the 24 week salt spray test, when compared to primer and CARC paint protection. However, the increased mass loss due to the resulting HAZ raises concerns at the exposed deposition interface.

From the work performed and the correlative results obtained, it is plausible to hypothesize that further optimization of the Stellite 6 coating to reduce this HAZ in high hard steel will enable additional performance improvements against corrosive environments. The resistant properties of the DED coating clearly demonstrated better performance when compared to their painted and uncoated counterpart, despite the lack of optimization. This DED coating does not however replace CARC in the area of chemical/biological protection and camouflage, which would still require a CARC layer to be placed on top of the DED coating and its own interaction study.

The similar hardness of the deposition is of particular interest as a potential meet impact performance requirements. However, due to the softening of the microstructure beneath the

deposition and the thickness of the HAZ, clear alterations to the process controls used to produce the deposition are necessary to retain the substrate's desired mechanical properties. This HAZ was also concluded to require reduction as it demonstrated an increased susceptibility to mass loss. Porosity was also noted as an issue with the DED process parameters used for this preliminary study. Optimization of the process controls shall be focused on the reduction of these types of defects for applicable use of the coating.

## 6. REFERENCES

(Note: Use IEEE style)

- [1] J.C. Shin, J.M. Doh, J.K. Yoon, "Effect of molybdenum on the microstructure and wear resistance of cobalt-base Stellite hardfacing alloys," 2003, Surface and Coatings Technology, 117-126
- [2] Deloro Group, "Stellite 6 Alloy", (Technical Report, Deloro Stellite, 2012)
- [3] Md.S. Hasan, Md.A. Mazid, R.E Clegg, Hasan et al. (2016): International Journal of Engineering Materials and Manufacture, 1(2), 35-50
- [4] Kennametal Inc., "Corrosion Resistance", (Technical Report, Kennametal Inc.)
- [5] Granta Design, AISI 4140, (2019) CES Selector 2019-MaterialUniverse
- [6] US Army, "DETAIL SPECIFICATION-ARMOR PLATE, STEEL, WROUGHT, HIGH-HARDNESS", 2015, MIL-DTL-46100E